

## Pulmonary Computed Tomography Hallmarks and the Short-term Outcome of COVID-19 Pneumonia in Patients with an Underlying Cardiovascular Disease

Nahid Rezaeian <sup>1</sup>, Parham Rabiei <sup>1</sup>, Shirin Manshouri <sup>2</sup>, Leila Hosseini <sup>1,3</sup>, Yaser Toloueitabar <sup>4</sup>, Marzieh Motevalli <sup>1</sup>, Hamidreza Pouraliakbar <sup>1</sup>, Leila Shayan <sup>5</sup>, Sanaz Asadian <sup>1\*</sup>

**Nahid Rezaeian <sup>1</sup>**

Department of Radiology, Rajaie Cardiovascular Medical and Research Center, Iran University of Medical Sciences, Tehran, Iran.

**Parham Rabiei <sup>1</sup>**

Department of Radiology, Rajaie Cardiovascular Medical and Research Center, Iran University of Medical Sciences, Tehran, Iran.

**Shirin Manshouri <sup>2</sup>**

Rajaie Cardiovascular Medical and Research Center, Iran University of Medical Sciences, Tehran, Iran.

**Leila Hosseini <sup>1,3</sup>**

Department of Radiology, Rajaie Cardiovascular Medical and Research Center, Iran University of Medical Sciences, Tehran, Iran.

Cardiology Department, North Khorasan University of Medical Sciences, Bojnurd, Iran.

**Yaser Toloueitabar <sup>4</sup>**

Department of Congenital Cardiac Surgery, Rajaie Cardiovascular Medical and Research Center, Iran University of Medical Sciences, Tehran, Iran.

**Marzieh Motevalli <sup>1</sup>**

Department of Radiology, Rajaie Cardiovascular Medical and Research Center, Iran University of Medical Sciences, Tehran, Iran

**Hamidreza Pouraliakbar <sup>1</sup>**

Department of Radiology, Rajaie Cardiovascular Medical and Research Center, Iran University of Medical Sciences, Tehran, Iran

**Leila Shayan <sup>5</sup>**

Trauma Research Center, Rajaee (Emtiaz) Trauma Hospital, Shiraz University of Medical Sciences, Shiraz, Iran

**Sanaz Asadian <sup>1\*</sup>**

Department of Radiology, Rajaie Cardiovascular Medical and Research Center, Iran University of Medical Sciences, Tehran, Iran

\*Email: asadian\_s @ yahoo.com; asadian\_s @ rhc.ac.ir

### Abstract

#### **Background:**

The reference laboratory examination for the diagnosis of coronavirus disease 2019 (COVID-19) is the reverse transcription-polymerase chain reaction (RT-PCR) test; nonetheless, given its false-negative results, chest computed tomography (CT) is deemed a worthier method. We aimed to define the chest

CT characteristics of patients with COVID-19 who suffered from an underlying cardiovascular disease (CVD) and determine the correlation between short-term clinical outcomes and imaging features.

**Results:**

Our retrospective cross-sectional study registered 36 patients with definitive COVID-19 pneumonia suffered from an underlying CVD. For all the patients, imaging and laboratory evaluations were done within 3 to 6 days from symptom onset. Imaging and lab findings and short-term clinical outcomes were recorded and analyzed. In our population (mean age of  $51.22 \pm 20.59$  years), 20 (55.6%) patients improved and 16 (44.4%) expired. The most frequent pulmonary parenchymal patterns were ground-glass opacity (GGO) (97.2%, 35/36), pulmonary arterial focal dilatation (72.2%, 26/36), consolidation (63.9%, 23 /36), and bronchial wall thickening (63.9%, 23/36). The mortality rate was higher in the presence of the crazy-paving pattern (72.7%, 8 /11), multilobar lung disease (53.8%, 14/26), and lobar pulmonary involvement (100%, 5/5) (all  $P$ s < 0.05). The median of the total severity score (TSS) was higher in the non-surviving patients ( $P = 0.06$ ).

**Conclusions:**

The most common CT features were GGO, pulmonary arterial focal dilatation, consolidation, and bronchial wall thickening. The crazy-paving pattern, multilobar involvement, lobar pneumonia, higher TSS, and also particular CT characteristics in CVD cases with anemia and lymphopenia were significant indicators of mortality.

**Keywords:** Cardiovascular Disease, Clinical Outcome, COVID-19, Lung Computed Tomography.

**Introduction**

Coronavirus Disease 2019 (COVID-19) is an extremely contagious infection that provokes severe acute respiratory syndrome coronavirus 2 (SARS-CoV-2). With its origins in China, COVID-19 spread throughout the world within several months [1]. A spectrum of manifestations, from mild to severe symptoms, is demonstrable. SARS-CoV-2 uses angiotensin-converting enzyme-2 to enter different human cells, causing interstitial lung injury and, consequently, parenchymal damage [2].

COVID-19 may disproportionately influence subjects with an underlying cardiovascular disease (CVD) [3]. An essential reference laboratory examination for COVID-19 is the reverse transcription-polymerase chain reaction (RT-PCR) test, although several cases of false-negative results have been published. Given the limitation of RT-PCR, chest CT scanning is considered a valuable method in the diagnosis of this group of patients [4-6]. On account of its strengths, chest CT is regarded as the most reliable imaging technique for the evaluation of COVID-19. Further, based on the Diagnosis and Treatment Program (6th edition), presented by the National Health Commission of China, the CT method plays a key role in recognizing COVID-19, monitoring its progression, and appraising the therapeutic effectiveness [7]. The principal manifestation of COVID-19 in chest CT is bilateral ground-glass opacity (GGO), frequently in the posterior and peripheral portions of the lung [8,9]. Nonetheless, with the increase in the number of cases, a spectrum of findings has been detected in CT that includes the crazy-paving pattern, pulmonary arterial focal dilation, and airway disease [10-12].

We sought to define the CT features in patients with COVID-19 who suffer from an underlying CVD and to investigate whether there was a connection between short-term clinical outcomes and imaging features in the early stage of the illness [13].

**Methods**

**Patient selection**

This retrospective cross-sectional study obtained approval from the Review Board and Ethics Committee of Rajaie Cardiovascular Medical and Research Center. The study population consisted of 36 patients with a definitive diagnosis of COVID-19 based on positive RT-PCR and evidence of respiratory involvement in chest CT scans [5], in combination with clinical manifestations. CT images

were obtained from all these patients between March 2020 and June 2020. The patients were stable before hospitalization and underwent routine clinical follow-ups.

The entire study population underwent both imaging and laboratory evaluations within 3 to 6 days from symptom onset. At least 1 imaging examination was performed for each patient; in the case of 2 or more studies, the first study was interpreted. The imaging and laboratory evaluations were both on the same day.

Underlying CVDs included ischemic and nonischemic cardiomyopathies, valvular heart diseases, congenital heart diseases, and cardiac transplantation. The patients' outcomes during hospitalization were recorded based on recovery and discharge from the hospital or inpatient mortality.

### **CT Characteristics**

CT images were obtained with a Siemens SOMATOM scope 16-slice multidetector scanner. A low-dose pulmonary CT without utilizing a contrast medium was applied. Image acquisition parameters were as follows: a tube voltage of 120 KVp, a tube current of 70 to 80 mAs, and a slice thickness of 3 mm at a 10-mm slice interval. A 1.5-mm high-resolution algorithm was used to reconstruct the lung window. The mean CT dose index volume was 4.1 mGy (range: 3–6.3 mGy). All the CT images were interpreted in both lung (width: 1500 HU, level: –600 HU) and mediastinal (width: 350 HU, level: 50 HU) windows by 2 different expert radiologists separately. In case of conflict in opinions, the final comment stated by a third, more experienced, radiologist.

### **Patterns of Lung Involvement**

GGO is considered an ill-defined region in the lung caused by the partial airspace filling and thickening of the interstitium that does not lead to the obscuration of the vascular and bronchial boundaries [14].

Consolidation is defined as alveolar air replaced by pathological substances such as cells, tissues, and liquids; it manifests itself as an increased density in the pulmonary parenchyma and results in the obscuration of the borders of the underlying vessels and the airway walls [14].

Vascular enlargement is defined as the dilatation of the pulmonary vascular structures surrounding or inside the lesion [15].

The crazy-paving pattern is manifested as thickened interlobular septa and intralobular lines on an underlying GGO, resembling asymmetrical paving stones [14,16].

The halo sign is defined as nodules encircled by GGO [14].

The reticular pattern is defined as the thickening of the interstitial lung parenchyma including the interlobular septa and intralobular lines [14,17] and is displayed with a spectrum of small lines in chest CT [18].

In the present study, fibrosis, subpleural sparing, pleural effusion, pericardial effusion, mediastinal or hilar lymphadenopathy, emphysematous changes, cavitation or nodule formation, associated pulmonary thromboembolism, the tree-in-bud pattern, the reverse halo sign, and bronchial wall thickening were defined based on the latest guidelines [15,19].

### **Localization of Lung Involvement**

In the current investigation, the distribution of the parenchymal involvement was described as transverse (central, peripheral, and nonspecific) and longitudinal (upper lobe, middle lobe, lower lobe, and multilobar). The pattern of pulmonary engagement was classified as segmental and lobar, and the laterality of involvement was defined as bilateral, right-sided, and left-sided. The central lung portion was considered the inner two-thirds of the pulmonary parenchyma, while the peripheral part was defined as the outer one-third of the lung. The TSS of the parenchymal involvement was calculated for each patient [20]. The mentioned data were classified based on the affected volume and the score as follows: none (0%, 0), minimal (1%–25%, 1), mild (26%–50%, 2), moderate (51%–75%, 3), and severe (76%–100%, 4). Eventually, TSS was quantified by summing the 5 lobe scores (range of scores: 0–20).

### Laboratory Findings

Laboratory parameters, including total white blood cells, the lymphocyte count, and hemoglobin (Hb), were evaluated. The patients were divided based on their lymphocyte count as higher than 1100/ $\mu$ L and equal or lower than 1100/ $\mu$ L. The latter was considered to represent lymphopenia. Additionally, anemia was considered a maximum Hb level of 12 g/dL.

### Statistical Analysis

The categorical variables were displayed as frequencies and percentages, while the continuous variables were reported as the mean  $\pm$  the standard deviation (SD) or the median with the interquartile range (IQR) depending on the normality of the distribution. The differences between the groups were analyzed using the  $\chi^2$  test for the categorical variables and the ANOVA test for the continuous variables. The mean values were compared using a 2-sample *t*-test. In the presence of non-normal distributions, nonparametric tests, including the Mann–Whitney and Kruskal–Wallis tests were used. All the statistical analyses were conducted with the SPSS software, version 20.0 (IBM Corp), and a *P* value of less than 0.05 was considered statistically significant.

### Results

The study population was comprised of 36 patients, 24 (66.7%) male and 12 (33.3%) female, at a mean age of  $51.22 \pm 20.59$  years. The most frequent pulmonary parenchymal involvement patterns were GGO (97.2%, 35/36) (Fig. 1), pulmonary arterial focal dilatation (72.2%, 26/36) (Fig. 2), consolidation (63.9%, 23/36) (Fig. 3), and bronchial wall thickening (63.9%, 23/36). Table 1 shows the demographic and common chest CT characteristics of our study population.

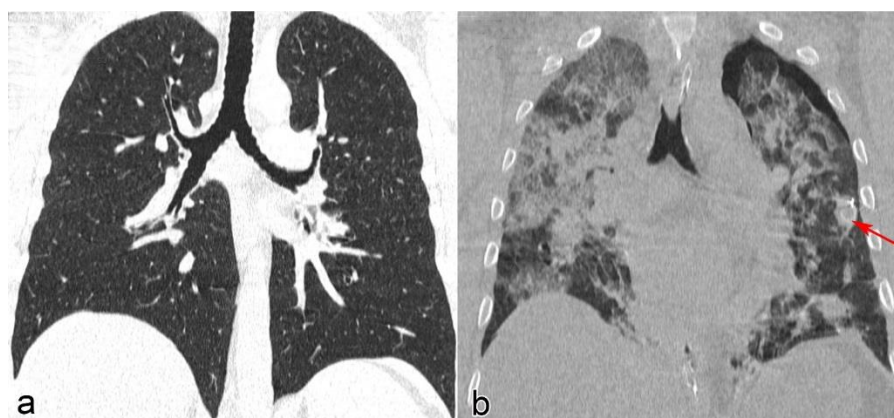


**Figure 1.** Unenhanced chest CT of a 50-year-old COVID-19 pneumonia patient with positive history of ischemic cardiomyopathy. Patchy segmental peripheral ground-glass opacity (arrow) and subpleural sparing (arrowhead) are the remarkable features. This patient successfully managed and discharged from hospital.



**Figure 2.** Unenhanced chest CT of a 38-year-old woman with newly diagnosed hypertrophic cardiomyopathy with confirmed COVID-19 pneumonia. Mild dilatation of the pulmonary arterial branches (arrowheads) traversing the region of segmental peripheral ground-glass density is evident.

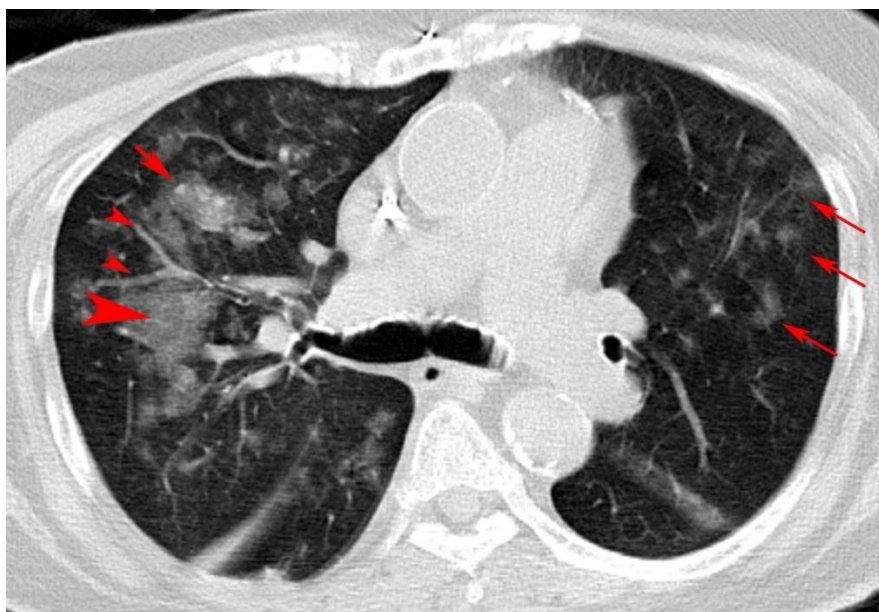


**Figure 3.** Unenhanced chest CT of a 48-year-old woman, known case of aortic valve stenosis, with confirmed COVID-19 pneumonia. Multi focal patchy segmental bilateral consolidations (arrowheads) are noted in both central and peripheral distribution.

Other findings consisted of pleural effusion (50%, 18/36), the crazy-paving pattern (30.6%, 11/36) (Fig. 4), halo appearance (30.6%, 11/36), reticular opacities (25%, 9/36), fibrosis (25%, 9/36), tree-in-bud opacities (13.9%, 5/36), pulmonary emphysematous changes (11.1%, 4/36), nodule formation (11.1%, 4/36), pericardial effusion (5.6%, 2/36), and lymphadenopathy (5.6%, 2/36). **Subpleural** stripe sparing was noted in 55.6% (20/36) of the patients (Fig. 1). None of the patients exhibited a reverse halo pattern, cavitation formation, or associated pulmonary thromboembolism. Table 2 presents the frequency of the common chest CT findings in our different CVD subgroups.

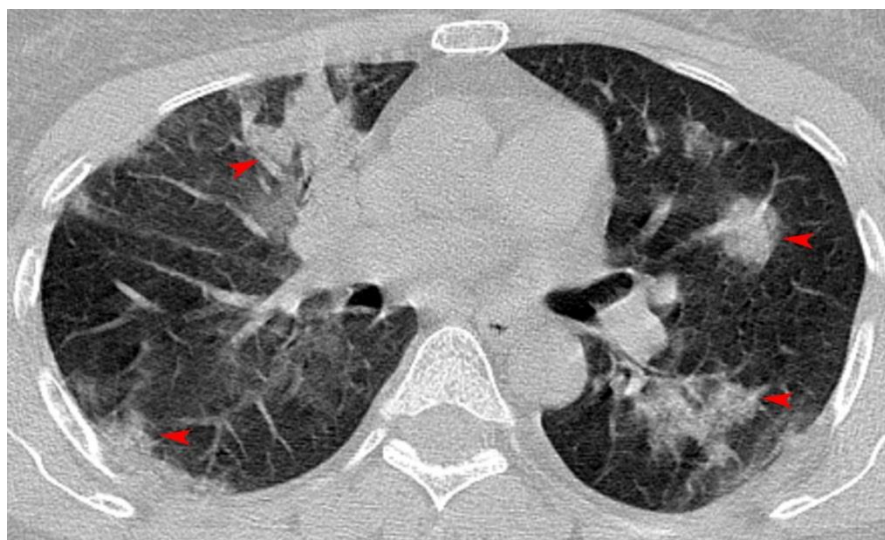


**Figure 4.** Unenhanced chest CT of a 72-year-old man with ischemic cardiomyopathy and proven COVID-19, complaining of grave respiratory symptoms. Note a combination of ground-glass opacities (long arrows), consolidation (short arrow), focal pulmonary arterial dilatation in the affected area (small arrowheads), and crazy-paving appearance (large arrowhead). The lesions are in both central and peripheral distribution. Sadly, this patient eventually expired.

**Table 1:** Demographic and common chest CT characteristics of the study population.

|  |   |
|--|---|
| Total number of patients                 | 36  |
| Gender                                   | Male: 66.7% (24/36)<br>Female: 33.7% (12/36)  |
| Mean age $\pm$ SD                        | 51.22 $\pm$ 20.59   |
| Major underlying CVD                     | Valvular Heart diseases: 13.9% (5/36)<br>Ischemic Cardiomyopathy: 38.9% (14/36)<br>Non-Ischemic cardiomyopathy: 25% (9/36)<br>Congenital Heart Diseases: 8.3% (3/36)<br>Cardiac Transplantation: 8.3% (3/36)<br>Others: 5.6% (2/36) |
| The most common CT patterns              | Ground-Glass Opacity: 97.2% (35/36)<br>Pulmonary Arterial Focal Dilatation: 72.2% (26/36)<br>Consolidation: 63.9% (23/36)<br>Bronchial Wall Thickening: 63.9% (23/36)<br>Pleural effusion: 50% (18/36)                              |
| Laterality of pulmonary involvement      | Bilateral: 86.1% (31/36)<br>Isolated right side pneumonia: 8.3% (3/36)<br>Isolated left lung pneumonia 5.6% (2/36)  |
| Longitudinal distribution of the lesions | Multilobar: 72.2% (26/36)<br>Lower lobe: 16.7% (6/36)<br>Upper lobe: 8.3% (3/36)<br>Middle lobe: 2.8% (1/36)  |
| Transverse distribution of the lesions   | Central and Peripheral: 52.7% (19/36)<br>Peripheral: 47.2% (17/36)<br>Central: 0% (0/36)  |

CT: Computed Tomography, SD: Standard Deviation, CVD: Cardiovascular Disease

**Table 2:** The frequency of the common chest CT findings in different CVD subgroups



| Major Underlying CVD        | Pulmonary parenchymal CT finding |                     |               |                           |
|-----------------------------|----------------------------------|---------------------|---------------|---------------------------|
|                             | Ground-Glass Opacity             | Arterial dilatation | Consolidation | Bronchial wall thickening |
| Valvular heart diseases     | 100% (5/5)                       | 60% (3/5)           | 40% (2/5)     | 80% (4/5)                 |
| Ischemic cardiomyopathy     | 92.9% (13/14)                    | 64.3% (9/14)        | 42.9% (6/14)  | 42.9% (6/14)              |
| Non-ischemic cardiomyopathy | 100% (9/9)                       | 100% (9/9)          | 100% (9/9)    | 88.9% (8/9)               |
| Congenital heart diseases   | 100% (3/3)                       | 66.7% (2/3)         | 66.7% (2/3)   | 66.7% (2/3)               |
| Cardiac transplantation     | 100% (3/3)                       | 66.7% (2/3)         | 66.7% (2/3)   | 33.3% (1/3)               |
| Others                      | 100% (2/2)                       | 50% (1/2)           | 100% (2/2)    | 100% (2/2)                |

CT: Computed Tomography, CVD: Cardiovascular disease

Thirty-one (86.1%) patients had segmental involvement (Fig. 3). The lobar pattern was noted in 5 (13.9%) patients (Fig. 5). Bilateral pulmonary parenchymal involvement was evident in 31 (86.1%) patients; 8.3% (3/36 patients) had only right and 5.6% (2/36 patients) had only left lung pneumonia. Multilobar involvement was detected in 26 (72.2%) patients, lower lobe involvement in 6 (16.7%), upper lobe involvement in 3 (8.3%), and middle lobe involvement in 1 (2.8%).

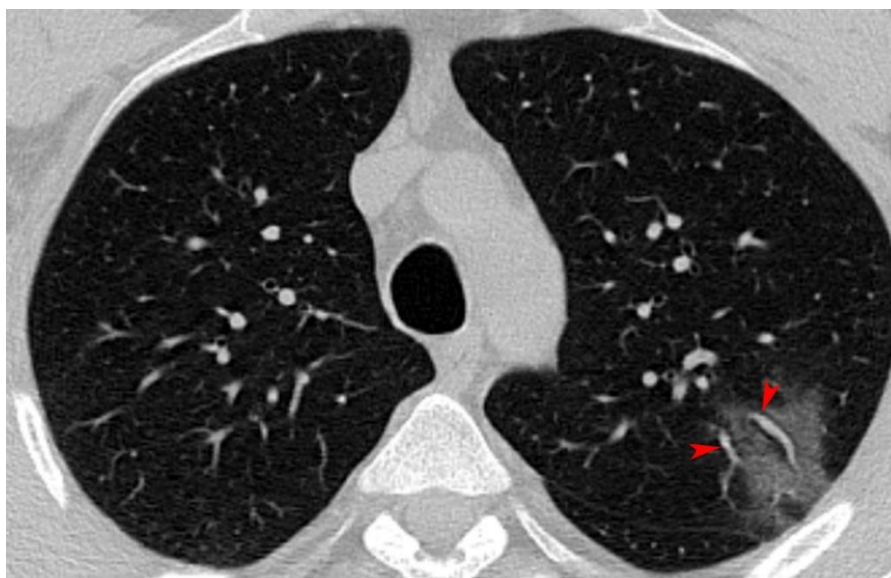


**Figure 5.** Unenhanced chest CT of a 62-year-old case of ischemic cardiomyopathy with documented COVID-19 and severe respiratory manifestations; lobar pneumonia with known “air-bronchogram sign” (arrows) was evident. Unfortunately, this patient expired.

Both central and peripheral pulmonary involvement was detected in 52.7% (19/36) of the patients, and 47.2% (17/36) had only peripheral pneumonia. Isolated central lung disease was noted in none of the patients.

Complete improvement was detected in 20 (55.6%) patients, and 16 (44.4%) patients unfortunately expired (Table 3). There were no significant differences in the mean of age between the recovered and non-surviving groups.

**Table 3.** COVID-19 pneumonia outcome in different groups of CVD patients

|          | Major underlying CVD    |                         |                             |                           |                    |                 | Total      |
|----------|-------------------------|-------------------------|-----------------------------|---------------------------|--------------------|-----------------|------------|
|          | Valvular heart diseases | Ischemic cardiomyopathy | Non-ischemic cardiomyopathy | congenital heart diseases | Cardiac transplant | Other disorders |            |
| Improved | 3 (60.0%)               | 8 (57.1%)               | 3 (33.3%)                   | 3 (100.0%)                | 2 (66.7%)          | 1 (50.0%)       | 20 (55.6%) |
| Expired  | 2 (40.0%)               | 6 (42.9%)               | 6 (66.7%)                   | 0 (0.0%)                  | 1 (33.3%)          | 1 (50.0%)       | 16 (44.4%) |
| Total    | 5 (13.9%)               | 14 (38.9%)              | 9 (25.0%)                   | 3 (8.3%)                  | 3 (8.3%)           | 2 (5.6%)        | 36 (100%)  |

CVD: Cardiovascular Disease

The mortality rate was higher in the group with a positive CT scan for consolidation (52.2%, 12/23) than in the group with a negative CT scan for consolidation (30.8%, 4/13); this difference, however, did not constitute statistical significance ( $P = 0.3$ ). The same result was observed in the presence of bronchial wall thickening in the CT scan.

The mortality rate was 72.7% (8/11) in the patients with a positive crazy-paving pattern and 32% (8/25) in those with a negative crazy-paving pattern; the difference was statistically significant ( $P = 0.03$ ).

The mortality rate was 57.9% (11/19) in the patients with the involvement of both central and peripheral pulmonary parenchyma and 29.4% (5/17) in those with the involvement of only the peripheral pulmonary parenchyma; nevertheless, the difference was not meaningful statistically ( $P = 0.1$ ). The rate of mortality was 53.8% (14/26 cases) in the patients with multilobar lung disease and 33.3% (2/6) in those with only lower lobar involvement. None of the patients with upper or middle lobar engagement died; these differences were statistically significant ( $P = 0.04$ ). Notably, all 5 patients with lobar pulmonary involvement expired ( $P = 0.01$ ).

The mortality rate was 48.4% (15/31) for bilateral pneumonia, 33.3% (1/3) for isolated right-sided pneumonia, and 0% for the involvement of only the left lung, although these ratios were not significant statistically ( $P = 0.1$ ).

The recovered group had a severity score median of 6 and a severity score IQR of 5, whereas the non-surviving group had a severity score median of 8 and a severity score IQR of 7; the difference between the 2 groups vis-à-vis the severity score median was statistically relatively significant ( $P = 0.06$ ).

Consolidation was observed in 75% (15/20) of the patients with anemia and 50% (8/16) of those without it, which was not statistically significant ( $P = 0.1$ ). Among the patients with anemia, 35% (7/20) had a crazy-paving pattern in the CT scan, while this ratio was 25% (4/16) for the group with normal Hb levels ( $P = 0.7$ ). In the anemic group, the proportion of the patients with pericardial effusion in the chest CT scan was 10% (2/20), while none of the patients in the non-anemic group had pericardial effusion; the difference was not statistically meaningful ( $P = 0.4$ ). Multilobar engagement was detected in 75% (15/20) of the patients with anemia and 68.8% (11/16) of those with normal Hb levels ( $P = 0.8$ ). A statistically significant correlation was noted ( $P = 0.05$ ) concerning the ratio of lobar lung disease in the anemic group (25%, 5 cases) versus the non-anemic group (0%). The mean of TSS was  $8.75 \pm 4.67$  in the anemic group and  $6.19 \pm 2.40$  in the non-anemic group, which showed a statistically significant difference ( $P = 0.04$ ).

Consolidation was detected in 75% (12/16) of the patients with low lymphocyte count (LLC) and 55% (11/20 cases) of those with high lymphocyte count (HLC), with the difference failing to reach statistical significance ( $P = 0.3$ ). The crazy-paving pattern was seen in the CT scan of 43.8% (7/16) of the patients with LLC and only 20% (4/20) of those with HLC; the difference was nonsignificant ( $P = 0.1$ ). The halo sign was noted in the chest CT scan of 18.8% (3/16) of the LLC group and 40% (8/20) of the HLC group ( $P = 0.2$ ). Chest CT scan findings of subpleural sparing was detected in 37.5% (6/16) of the LLC



group and 70% (14/20) of the HLC group ( $P = 0.09$ ). Focal vascular dilatation in the area of parenchymal involvement was seen in 62.5% (10/16) of the patients with LLC and 80% (16/20) of the patients with HLC ( $P = 0.2$ ). The proportion of visible pleural effusion was 55% (11/20) in the HLC group and 43.8% (7/16) in the LLC group ( $P = 0.7$ ), and the proportion of visible pericardial effusion was 10% (2/20) in the HLC group and 0% in the LLC group ( $P = 0.4$ ). None of the patients with HLC showed mediastinal or hilar lymphadenopathy, while 12.5% (2/16) of those with LLC did ( $P = 0.1$ ). Simultaneous central and peripheral lung involvement was seen in 68.8% (11/16) of the LLC group and 40% (8/20) of the HLC group ( $P = 0.1$ ). Multilobar lung disease was observed in 81.3% (13/16) of the patients with LLC and 65% (13/20) of those with HLC ( $P = 0.3$ ). Lobar involvement was noted in 18.8% (3/16) of the LLC group and 10% (2/20) of the HLC group ( $P = 0.6$ ). Bilateral lung disease was detected in 93.8% (15/16) of the patients with LLC and 80% (16/20) of those with HLC ( $P = 0.4$ ). The mean of TSS was  $9 \pm 3.74$  in the LLC group and  $6.50 \pm 3.94$  in the HLC group, which showed a relatively meaningful difference ( $P = 0.06$ ).

## **Discussion**

Patients with established COVID-19 pneumonia have typical imaging characteristics, which may be effective in the early screening of extremely suspected cases and in assessing the severity and degree of the disease [5]. We evaluated stable patients with an underlying CVD who suffered from COVID-19 pneumonia and analyzed imaging features and their correlation with clinical outcomes and some laboratory findings.

The main findings in our investigation were as follows:

1. The most common CT scan patterns were GGO, pulmonary arterial focal dilatation, consolidation, and bronchial wall thickening.
2. Bilateral, multilobar, and segmental pneumonia cases were noted more frequently than unilateral, unilobar, and lobar infection cases, respectively.
3. The mortality rate was 44% in our patient population.
4. The crazy-paving pattern, multilobar involvement, lobar (versus segmental) pneumonia, and a higher TSS were significant markers of mortality (Fig. 6).
5. The incidence of lobar pneumonia and the mean of TSS were notably higher in patients with anemia than in those with normal Hb levels.
6. The mean of TSS was significantly higher in patients with LLC than in those with HLC.

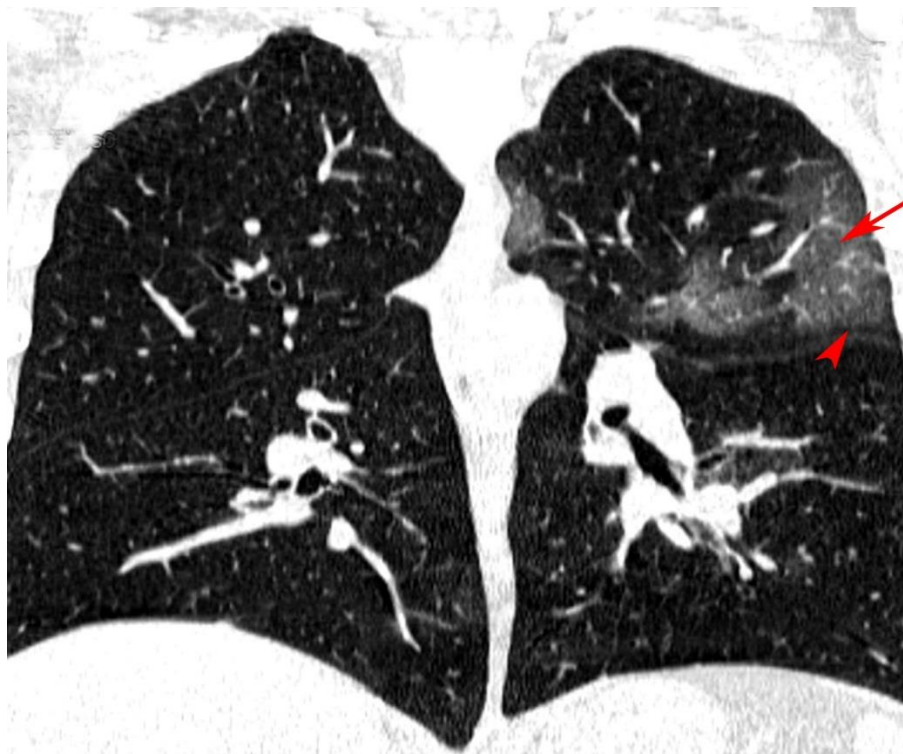


**Figure 6.** Unenhanced chest CT scan of a 49-year-old man, known case of non-ischemic dilated cardiomyopathy. (A), coronal view in the parenchymal window. The study had been done a month before manifestations of COVID-19 pneumonia, due to non-specific symptoms; it reveals normal pulmonary parenchyma. (B), the same view on admission with confirmed COVID-19 lung involvement; Note the extensive bilateral, multilobar, both central and peripheral parenchymal disease. Ground-glass opacity, consolidation, and crazy-paving appearance are present altogether. The calculated total severity score for this patient was 16/20. Left side pneumothorax appears to be an iatrogenic complication of chest tube insertion (arrow). The clinical condition of the patient exacerbated, and he died on day 4 of admission.

We found that GGO was the most frequent parenchymal involvement pattern (97.2%), which chimes in with the findings of a review article by Kunhua et al [21], who reported GGO in 98% of their patients with COVID-19 who did not suffer from an underlying CVD. Pulmonary arterial focal dilatation was a remarkable finding in our research (72.2%). A similarly notable finding (71.3%), probably caused by an inflammatory reaction, was reported in an investigation by Zhao et al [22]. We observed consolidation in the CT scan of 63.9% of our study population. The patients with consolidation had a higher, albeit nonsignificantly, mortality rate. Other studies have reported incidence rates of between 2% and 64% [11,21,23]. This finding could be a consequence of GGO progression or coexistence with GGO in 1 to 3 weeks [24].

Interestingly, the rate of bronchial wall thickening was high in our patient population in comparison with other investigations on patients without an underlying CVD (63.9% vs. 10-20% of the cases) [21,23]. A study by Li et al on 83 patients with COVID-19 demonstrated that thickened bronchial wall was significantly higher in critical patients than in less severe cases. Consequently, we believe that a previous history of CVD is a marker of a perilous condition [21].

The mortality rate in our study was extremely notable (44%). Our results indicated that the crazy-paving pattern (positive in one-third of our patients) was a significant marker of mortality. Therefore, in line with other studies [16], we conclude that the existence of a crazy-paving pattern may be an ominous sign of the onset of progressive or peak-stage COVID-19.

Our findings highlighted a strong correlation between multilobar involvement and worsened outcomes in patients with COVID-19 who suffered from an underlying CVD. We also observed a strong correlation between lobar involvement and mortality in that all our patients with lobar pneumonia died.

A relatively significant correlation between TSS and a poor outcome is found in our investigation. Xiong et al. showed the importance of TSS calculation for the quick detection of COVID-19 and standardized treatment and isolation [13]. Our results reinforce the role of TSS estimation not only in the initial diagnosis and clinical follow-up but also in the prediction of patients' outcome, especially for those with an underlying CVD.

Additional findings of CT in our subjects with COVID-19 included fibrosis or fibrous stripes (25%) and pleural effusion (50%). Some studies have reported a correlation between these findings and a poorer prognosis [16,21,24,25,26]; however, our results revealed no such association.

We detected the halo sign and subpleural sparing more frequently in patients with HLC than in those with LLC, which may denote a better immune response.

A powerful finding of our investigation was the correlation between the ratio of lobar lung disease and anemia. Considering the prognostic role of TSS, we compared the mean of TSS between anemic and non-anemic groups as well as LLC and HLC groups, which revealed a significant difference. We conclude that the existence of anemia and LLC correlates with worsened outcomes in the context of CVD.

Despite our remarkable results, the small number of cases in CVD subcategories precluded us from performing a subgroup analysis. This shortcoming can be addressed in large-scale multicentric research. Also, we plan to continue data collection in COVID-19 CVD patients with ongoing more researches confirming the grave course of the disease in CVD context and its impacts on the cardiovascular system [27].

### **Conclusions**

In conclusion, the most common CT characteristics in certain COVID-19 pneumonia cases suffering an underlying CVD were segmental GGO, pulmonary arterial focal dilatation, consolidation, and bronchial wall thickening in bilateral and multilobar arrangements. The existence of the crazy-paving pattern, multilobar involvement, lobar pneumonia, and a higher TSS was a significant indicator of fatality. Also, anemia and lymphopenia correlated with CT findings (higher TSS and lobar involvement), which in turn associated with higher mortality.

### **Declarations**

**Ethics approval and consent to participate:** All procedures performed in our study involving human participants were in accordance with the ethical standards of the institutional and national research committee and with the 1964 Helsinki Declaration and its later amendments or comparable ethical standards.

The study protocol was submitted to the ethics committee of our referring center. The need for informed consent waived by the ethics committee due to the retrospective design of the study. All the details that might disclose the identity of the subjects under study omitted.

**Consent for publication:** not applicable.

**Availability of data and material:** The datasets generated and analyzed during the current study are available from the corresponding author on reasonable request.

**Conflicts of interest/Competing interests:** The authors declare that they have no conflict of Interest related to the publication of this article.

**Funding:** No financial support was received for this study.

**Authors' contributions:** All authors: conception and design of the work; acquisition, analysis, and interpretation of the data for the work; drafting and revising the work; approval of the final version; and accountability for all aspects of the work.

### **Acknowledgments**

We would like to thank Dr. Hooman Bakhshandeh for his assistance in the study design and Dr. Pardis Moradnejad for her support in data collection.

### **Key Points**

- The most frequent chest CT patterns in COVID-19 patients with cardiovascular disease sought.
- Commonest features were ground-glass opacity, focal arterial dilatation, consolidation, and bronchial wall thickening.
- Bilateral, multilobar, and segmental pneumonia cases noted more commonly.
- Particular CT patterns associated with higher fatality.

### **Abbreviations**

CT: Computed Tomography, COVID-19: Coronavirus Disease 2019, RT-PCR: Reverse Transcription-Polymerase Chain Reaction, GGO: Ground-Glass Opacity, TSS: Total Severity Score, CVD: Cardiovascular Disease, HLC: High Lymphocyte Count, LLC: Low Lymphocyte Count.

### **Reference**

1. Zhu N, Zhang D, Wang W, Li X, Yang B, Song J, Zhao X, Huang B, Shi W, Lu R (2020) A novel coronavirus from patients with pneumonia in China, 2019. *New England Journal of Medicine*
2. Sun K, Chen J, Viboud C (2020) Early epidemiological analysis of the coronavirus disease 2019 outbreak based on crowdsourced data: a population-level observational study. *The Lancet Digital Health*
3. Guo T, Fan Y, Chen M, Wu X, Zhang L, He T, Wang H, Wan J, Wang X, Lu Z (2020) Cardiovascular implications of fatal outcomes of patients with coronavirus disease 2019 (COVID-19). *JAMA cardiology*
4. Fang Y, Zhang H, Xie J, Lin M, Ying L, Pang P, Ji W (2020) Sensitivity of chest CT for COVID-19: comparison to RT-PCR. *Radiology*:200432
5. Huang C, Wang Y, Li X, Ren L, Zhao J, Hu Y, Zhang L, Fan G, Xu J, Gu X (2020) Clinical features of patients infected with 2019 novel coronavirus in Wuhan, China. *The lancet* 395 (10223):497-506
6. Xie X, Zhong Z, Zhao W, Zheng C, Wang F, Liu J (2020) Chest CT for typical 2019-nCoV pneumonia: relationship to negative RT-PCR testing. *Radiology*:200343
7. COVID C situation report by February 29. National Health Commission of the People's Republic of China.
8. Chung M, Bernheim A, Mei X, Zhang N, Huang M, Zeng X, Cui J, Xu W, Yang Y, Fayad ZA (2020) CT imaging features of 2019 novel coronavirus (2019-nCoV). *Radiology* 295 (1):202-207
9. Wang D, Hu B, Hu C, Zhu F, Liu X, Zhang J, Wang B, Xiang H, Cheng Z, Xiong Y (2020) Clinical characteristics of 138 hospitalized patients with 2019 novel coronavirus-infected pneumonia in Wuhan, China. *Jama* 323 (11):1061-1069
10. Qian L, Yu J, Shi H (2020) Severe acute respiratory disease in a Huanan seafood market worker: Images of an early casualty. *Radiology: Cardiothoracic Imaging* 2 (1):e200033
11. Bernheim A, Mei X, Huang M, Yang Y, Fayad ZA, Zhang N, Diao K, Lin B, Zhu X, Li K (2020) Chest CT findings in coronavirus disease-19 (COVID-19): relationship to duration of infection. *Radiology*:200463
12. Fang Y, Zhang H, Xu Y, Xie J, Pang P, Ji W (2020) CT manifestations of two cases of 2019 novel coronavirus (2019-nCoV) pneumonia. *Radiology* 295 (1):208-209
13. Xiong Y, Sun D, Liu Y, Fan Y, Zhao L, Li X, Zhu W (2020) Clinical and high-resolution CT features of the COVID-19 infection: comparison of the initial and follow-up changes. *Investigative radiology*

14. Hansell DM, Bankier AA, MacMahon H, McLoud TC, Muller NL, Remy J (2008) Fleischner Society: glossary of terms for thoracic imaging. *Radiology* 246 (3):697-722
15. Ye Z, Zhang Y, Wang Y, Huang Z, Song B (2020) Chest CT manifestations of new coronavirus disease 2019 (COVID-19): a pictorial review. *European radiology*:1-9
16. Pan F, Ye T, Sun P, Gui S, Liang B, Li L, Zheng D, Wang J, Hesketh RL, Yang L (2020) Time course of lung changes on chest CT during recovery from 2019 novel coronavirus (COVID-19) pneumonia. *Radiology*:200370
17. Ajlan AM, Ahyad RA, Jamjoom LG, Alharthy A, Madani TA (2014) Middle East respiratory syndrome coronavirus (MERS-CoV) infection: chest CT findings. *American journal of roentgenology* 203 (4):782-787
18. Xu Z, Shi L, Wang Y, Zhang J, Huang L, Zhang C, Liu S, Zhao P, Liu H, Zhu L (2020) Pathological findings of COVID-19 associated with acute respiratory distress syndrome. *The Lancet respiratory medicine* 8 (4):420-422
19. Rossi SE, Franquet T, Volpacchio M, Giménez A, Aguilar G (2005) Tree-in-bud pattern at thin-section CT of the lungs: radiologic-pathologic overview. *Radiographics* 25 (3):789-801
20. McRae MP, Simmons GW, Christodoulides NJ, Lu Z, Kang SK, Fenyo D, Alcorn T, Dapkins IP, Sharif I, Vurmaz D (2020) Clinical decision support tool and rapid point-of-care platform for determining disease severity in patients with COVID-19. *Lab on a Chip*
21. Li K, Wu J, Wu F, Guo D, Chen L, Fang Z, Li C (2020) The clinical and chest CT features associated with severe and critical COVID-19 pneumonia. *Investigative radiology*
22. Zhao W, Zhong Z, Xie X, Yu Q, Liu J (2020) Relation between chest CT findings and clinical conditions of coronavirus disease (COVID-19) pneumonia: a multicenter study. *American journal of roentgenology* 214 (5):1072-1077
23. Wu J, Wu X, Zeng W, Guo D, Fang Z, Chen L, Huang H, Li C (2020) Chest CT findings in patients with coronavirus disease 2019 and its relationship with clinical features. *Investigative radiology* 55 (5):257
24. Shi H, Han X, Jiang N, Cao Y, Alwalid O, Gu J, Fan Y, Zheng C (2020) Radiological findings from 81 patients with COVID-19 pneumonia in Wuhan, China: a descriptive study. *The Lancet Infectious Diseases*
25. Pan Y, Guan H, Zhou S, Wang Y, Li Q, Zhu T, Hu Q, Xia L (2020) Initial CT findings and temporal changes in patients with the novel coronavirus pneumonia (2019-nCoV): a study of 63 patients in Wuhan, China. *European radiology*:1-4
26. Kong W, Agarwal PP (2020) Chest imaging appearance of COVID-19 infection. *Radiology: Cardiothoracic Imaging* 2 (1):e200028
27. Ranard LS, Fried JA, Abdalla M, Anstey DE, Givens RC, Kumaraiah D, Kodali SK, Takeda K, Karpaliotis D, Rabbani LE (2020) Approach to Acute Cardiovascular Complications in COVID-19 Infection. *Circulation: Heart Failure*.